

Article

Flexural Behavior of Epoxy under Accelerated Hygrothermal Conditions

Abulgasem Mohamed Elarbi and Hwai-Chung Wu *

Department of Civil and Environmental Engineering, Wayne State University, Detroit, MI 48202, USA; Arabi98@Yahoo.com

* Correspondence: hcwu@wayne.edu; Tel.: +1-313-577-0745

Academic Editor: Francesco Bencardino

Received: 21 April 2017; Accepted: 21 June 2017; Published: 7 July 2017

Abstract: Fibers by themselves have a limited use in engineering applications since they cannot transmit loads from one to another; therefore, the matrix material plays an important role in the overall function of the fiber reinforced polymer (FRP) composites. This paper intends to study the long term strength of epoxy resins subject to accelerated hygrothermal conditions. Such tests are able to predict the weather durability performance of epoxy materials, which is particularly important for many FRP bonded concrete structures. Several sets of epoxy beam specimens have been constructed and exposed to various hygrothermal environments (25 °C, 100 °C, 180 °C and 0% or 100% relative humidity). Specimens were then evaluated at selected thermal cycles by three-point flexural tests. The flexural strength, mid-span deflection, and stiffness, as well as the mode of failure, have been examined in this study.

Keywords: fiber reinforced polymer (FRP); resin; hygrothermal effect; accelerated test; strength deterioration

1. Introduction

Applications of FRP composites in civil/infrastructure engineering are diverse. Most applications involve externally bonded composite fabrics or jackets on beams, columns, and bridge decks. Significant improvements in the compressive, shear, and flexural behavior of bonded concrete elements have been obtained [1–4]. The performance of FRP bonded structures is highly affected by the bond characteristics, which depend, to a great extent, on the substrate condition to which FRP is bonded [5,6]. Good bonds are essential for the effectiveness of the composite action between the FRP and the concrete structure. In the case of non bond-critical applications such as confinement, with or without the use of resin [7], bonding is generally not of significance, but the weather durability of the FRP is still a major concern.

During the past decades, a large body of research has been directed towards better understanding the behavior of civil infrastructures employing FRP composites, and for the development of design guidelines. Nevertheless, these studies have generally ignored or marginally evaluated the reaction of structural systems using FRP to the environments, most importantly temperature changes, to which civil engineering structures are subjected [3,8]. Under everyday service conditions, FRP bonded structures are subjected to a wide range of temperature and moisture changes. The combination of environmental and mechanical loading complicates the durability assessment of an FRP composite.

Regarding bond failure, ASTM (American Society for Testing and Materials) D7522 [9] specifies the possible failure modes due to environmental degradation as being adhesive failure at the adhesive interface or, less likely, cohesive failure in concrete. Environmental conditions could also lead to a cohesive failure in the FRP laminate, which would represent a degradation of the FRP material itself, but this failure mode is usually expected when fibers are not completely wet-out. The desirable

failure on site is a cohesive failure in the concrete substrate, which represents a sound FRP-adhesive system. Mixed failures are also frequently found. This type of failure is expected to start cohesively in the concrete substrate, and then propagate throughout the interface, becoming adhesive [9]. Bond durability is critical to the overall integrity of the strengthening system and, consequently, to its long-term performance [6,10–13].

In addition to the bond problems, those failure modes of the FRP composites which are most likely to be affected by environmental conditions are the failure modes associated with the polymer matrix materials. Various environments may cause matrix deterioration or fiber-matrix interface deterioration. It has been reported that the moisture absorption of composite materials causes plasticization and hydrolysis through an attack on the ester linkage (group); both processes result in a higher induced molecular mobility, causing the deterioration of composites [14]. Micro-cracking in the matrix resin results in an increase of water absorption at higher temperatures followed by increased resin plasticization and hydrolysis [15].

Jones [16] and Pérez-Pacheco et al. [17] studied the effect of water and found that moisture diffusion into an epoxy matrix and the susceptibility of the fibers to water can cause changes in the thermophysical, mechanical, and chemical characteristics of FRPs. Moisture in the resin can weaken the Van der Waals force between the polymer chains and lead to a large reduction in bond strength. The swelling stress induced by the moisture uptake can also cause matrix cracking and fiber-matrix debonding [18]. A high temperature and high humidity are particularly detrimental [6]. Low to moderate heat may initially accelerate post curing, but moderate to high heat can quickly degrade epoxy resins. Furthermore, other synergistic effects of environmental conditions must also be addressed with care. For instance, FRP systems in contact with moisture and subjected to temperature cycles are expected to have a lower durability due to the deterioration of the bond between the concrete and FRP [6,19].

Birger et al. [19] reported that carbon/epoxy composites at 50 °C (106 °F) and at 95 percent relative humidity show almost no degradation in their mechanical properties. Haque et al. [20] also showed that the degradation of GFRP (Glass Fiber Reinforced Polymer) in terms of strength at temperatures below 100 °C (212 °F) is negligible, and that moisture degradation is less severe than temperature degradation.

Ouyang and Wan [21] modeled moisture transportation in the FRP strengthened concrete specimens by using relative humidity as a global variable. They derived a moisture diffusion governing equation for a multilayered composite. Based on their experimental and numerical results, they concluded that moisture accumulated at the interface mainly came from the bond free area close to the FRP and the sides of the concrete specimen. A highly uneven moisture distribution along the adhesive thickness was found, especially in the case of a relatively short period of exposure.

The effect of a hygrothermal environment on the performance of composites has been the subject of numerous investigations [11,22]. However, there is considerably less information on the accelerated laboratory characterization of the effect of environments on the polymeric resins as matrix materials of the composites. In polymer-matrix composites, the effects of a hygrothermal environment are primarily observed in the matrix properties. The strength of composites is closely related to the strength and orientations of the fibers. Nevertheless, the matrix properties have a fundamental effect on the damage resistance and durability of composites. Matrix properties are a deciding factor with respect to the location and nature of damage initiation, damage growth, and subsequent damage progression. For most composite structures, initial damage occurs in the matrix material as transverse tensile failure or shear failure, depending on the geometry and loading [23].

The effects of cold temperatures (freeze/thaw cycling) were previously found to cause insignificant changes in flexural strength and modulus for the composite specimens conditioned in distilled water and saltwater [24]. In this study, we focused on hot temperature environments to investigate the applications of FRP systems in many hot and humid regions around the world. This paper presents the results of an experimental study to quantify the effects of the hygrothermal

environments on the durability performance of epoxy materials. Rectangular epoxy beams have been constructed, cured, subjected to different environmental conditions, and tested for flexural responses. The temperature was varied from 25 °C, 100 °C and 180 °C (73 °F, 212 °F and 356 °F), while the humidity was 0 or 100%.

2. Experimental Program

2.1. Test Specimens

Sixty-nine epoxy beam specimens have been constructed. The total dimensions of each beam were 33 cm (13 in) long, 3.3 cm (1.3 in) wide, and 1.5 cm (0.6 in) thick. Rectangular molds have been used to cast these epoxy beam specimens. The molds constructed are consistent with ASTM D790-07 [25] standard test methods for the flexural properties of unreinforced and reinforced plastics and electrical materials; the effective length of these specimens was sixteen times that of the thickness.

2.2. Material Properties

A common two-component epoxy has been used in this study. It is a high elongation resin. The two components of part A and B are mixed in the ratio of 100:34.5 by weight, or 100 parts of component A to 42 parts of component B by volume. Table 1 shows the properties of this epoxy material.

Table 1. Epoxy mechanical properties (from the manufacturer's manual).

Curing Schedule 72 h Post Cure at 60 °C (140 °F)		
Property	ASTM	Typical Test Value
Glass Transition Temperature, T _g	D-4065	82 °C (180 °F)
Tensile Strength ¹	D-638	72.4 MPa (10,500 psi)
Tensile Modulus	D-638	3.18 GPa (461,000 psi)
Elongation (%)	D-638	5.0
Flexural Strength	D-790	123.4 MPa (17,900 psi)
Flexural Modulus	D-790	3.12 GPa (452,000 psi)

¹ Testing temperature 21 °C (70 °F).

2.3. Specimen Preparation and Curing

The two components (A and B) of the epoxy were mixed thoroughly. A mechanical drill equipped with a mixer beater was used to mix the two parts of the epoxy at low speed (400 rpm–600 rpm) until the mix became homogeneous. The mixing time was typically 5 min and the mixture was then cast in the molds. All of the specimens were cured in dry air under standard laboratory conditions for two weeks, where the temperature ranged from 23 °C–25 °C (70 °F–75 °F) and the relative humidity was between 22% and 25%, before they were exposed to the accelerated environmental conditions.

2.4. Accelerated Environmental Conditions

The influence of temperature on the mechanical properties of epoxy materials was the most important factor in this study. In addition to the room temperature, specimens had been exposed to two elevated temperatures (100 °C and 180 °C or 212 °F and 356 °F).

Relative humidity is another factor that was investigated in this research. Two levels of relative humidity have been used for this experimental work, 0% and 100%. Two furnaces with a maximum heat power range of 400 °C (752 °F), and two environmental chambers with a maximum temperature of 200 °C (392 °F), have been used for this purpose. The two furnaces were used for all samples conditioned at 0% humidity, while the two environmental chambers were used for the 100% humidity condition (Figure 1).



Figure 1. Environmental chamber (model: Tenny T10RC-1.5 SPL) (Tenny Engineering, 1090 SPRINGFIELD RD, Union, NJ 07083, United States).

To accelerate the hygrothermal effect on the specimens, the temperature was raised from room temperature to the specified value, kept at the specified temperature, and then returned to room temperature over a 2 h period (Figure 2). This is called the 2-h cycle regime. In addition, specimens were also conditioned at a constant temperature of 100 °C (called the zero cycle regime) to examine the effect of temperature cycling. Furthermore, selected specimens were stored in air under the standard laboratory conditions as the control group.

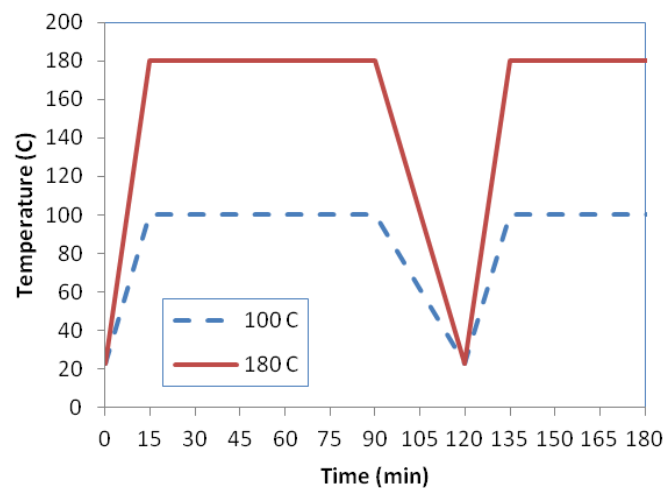


Figure 2. Temperature and humidity regime (2-h cycles).

2.5. Test Procedures

In this study, flexural tests were carried out to evaluate the deterioration rates after 0, 40, 100, 250, 350, and 625 thermal cycles.

All beams were tested by three-point bending. The effective length was 24.4 cm (9.6 in) for the center to center support. An MTS 810 machine (MTS Systems Corporation, 14000 Technology Drive,

Eden Prairie, MN 55344, USA) was used for the test; the rate of crosshead motion was calculated to be 0.1 mm/s based on ASTM [25].

$$R = \frac{ZL^2}{6d} \quad (1)$$

where: R is the rate of crosshead motion, mm (in)/min; L = support span, mm (in); d = depth of beam, mm (in); and Z = rate of starting of the outer fiber mm/mm/min, (in/in/min). Z shall equal 0.01.

3. Test Results

All of the specimens were subjected to a flexural test after being exposed to various environmental conditions. From these tests, the flexural strength, maximum center-point deflection, and apparent stiffness were deduced. All reported values represent the average of two tests.

It should be noted that all of the specimens, after being subjected to the designated high temperature conditioning, were not tested immediately after being removed from the ovens or the environmental chambers, but were left in air until they had cooled to room temperature before testing.

3.1. Control Specimens

Two specimens (EB0 and EB01) were considered as the control specimens; they were tested right after the completion of the standard curing period of 14 days. The mode of failure for these two control specimens was brittle flexural failure. The specimen split suddenly at the mid-span. The flexural load vs. deflection curves are shown in Figure 3.

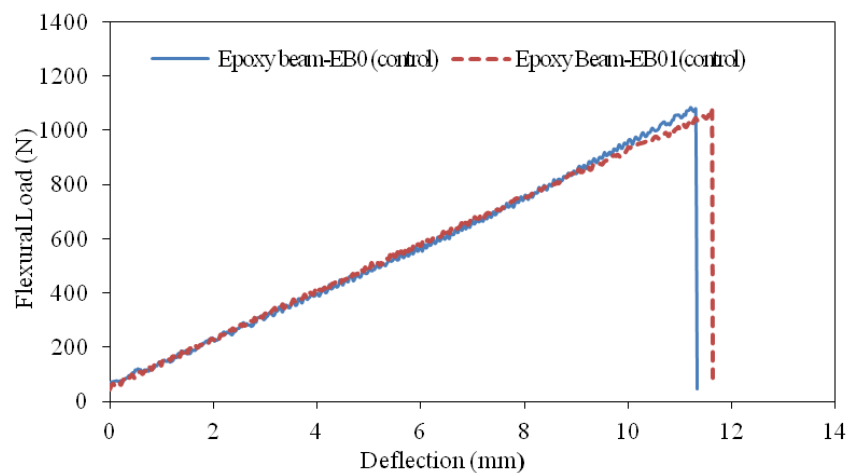


Figure 3. Flexural load-mid-span deflection curves of control epoxy beams.

Table 2 shows the test results of the control specimens, including the maximum flexural load, maximum flexural strength, maximum deflection at mid-span, apparent stiffness, and failure mode. All data of both specimens were close to each other. The stiffness of the specimens was calculated from the initial slope of the flexural load-deflection curves. The average of the maximum flexural loads of these two specimens was 1.08 kN (243.0 lbs).

Table 2. Test results of the epoxy control beam specimens.

Beam No.	Max. Deflection ⁺ (mm)	Max. Load (N)	Stiffness (N/mm)	Flexural Strength (MPa)	Failure Mode
EB0	11.4	1084.9	87.2	51.7	Flexural
EB01	11.6	1077.8	87.3	51.4	Flexural

⁺ mid-span deflection at the maximum load.

3.2. 100 °C Conditioned Specimens

3.2.1. 40 Cycles

Ten epoxy beams were subjected to different environmental cycling and tested after 40 cycles of 2-h period (80 h). Specimens EB1 and EB2 were left under the standard laboratory condition for 80 h, which is equivalent to 40 cycles of 2-h period. The remaining eight specimens were exposed to 100 °C and various conditions of relative humidity (RH) and cycle periods (Cp).

Compared to the control specimens, the flexural strength increased by 9% and the failure mode remained the same (brittle flexural failure) after 40 cycles (80 h) under the standard laboratory conditions. Other environmental conditions generally increased the flexural strength. In the case of 0% relative humidity, zero cycle tests improved the strength by 42%, while the 2-h cycle tests showed a 60% increase compared to the control. When the relative humidity was 100%, the strength increases were 74% and 53% for the zero cycle and the 2-h cycle specimens, respectively. It is noted that the zero cycle period refers to a constant 100 °C environment during the time of the conditioning. All but the zero cycle-0% humidity specimens show ductile failure (see Figures 4 and 5), while the latter showed the same brittle failure as the control.



Figure 4. Large deflection of the epoxy beam (EB10) after 40 Cycles at 100 °C.

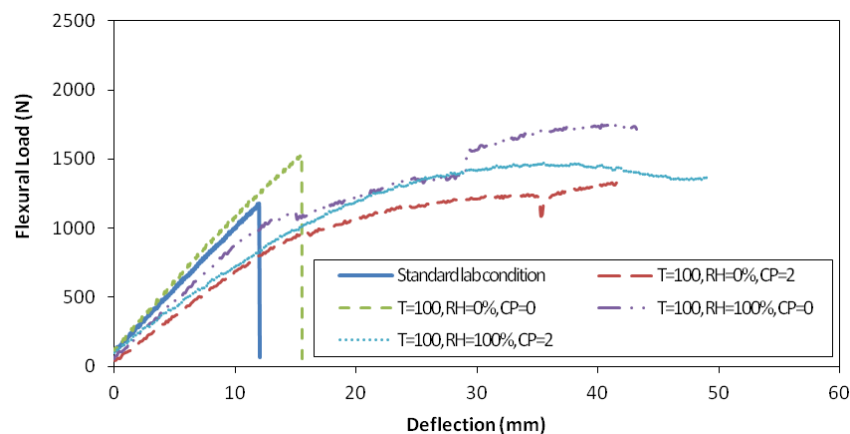


Figure 5. Flexural load-mid span deflection curves after 40 cycles under the conditions of 100 °C, humidity (0% and 100%), cycle period (Cp = 0 and 2).

3.2.2. 100 Cycles

After 100 cycles (200 h), the average maximum flexural load of the specimens EB3 and EB4, which were exposed to the standard laboratory condition, increased by 12.5% over the control specimens. Other environmental conditions generally increased the flexural strength over that of the corresponding 40 cycle specimens. For instance, under zero cycle-0% humidity, the increase in flexural strength reached 53.8% over the control specimens. Regarding the failure mode, all but one of the 2-h cycle-0% humidity specimens showed ductile failure. This other specimen behaved similarly until the peak load, at which point the specimen fractured completely (see Figure 6). Such a brittle failure was likely caused by the presence of a local defect. The flexural strengths of the zero-cycle specimens were larger than the two-hour cycle specimens either with or without moisture. More detailed comparisons will be given in the flexural strength section.

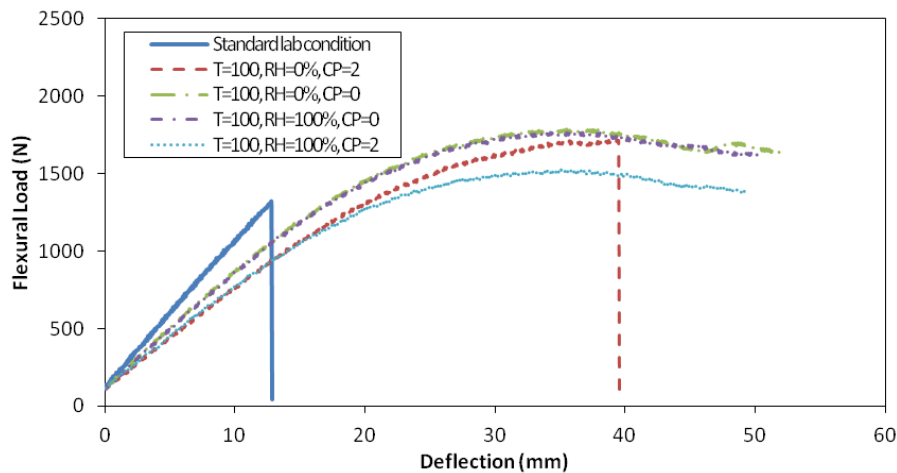


Figure 6. Flexural load-mid span deflection curves after 100 cycles under the conditions of 100 °C, humidity (0% and 100%), cycle period ($C_p = 0$ and 2).

3.2.3. 250 Cycles

By increasing the number of cycles to 250 (500 h), the increases in strength continued. For the standard laboratory condition specimens, the flexural strength at failure increased by 37.3% over the control specimens; the mode of failure remained brittle flexural failure. On the other hand, after 250 cycles of environmental conditioning at 100 °C, all eight specimens showed a large deformation without any failure. Tests then had to be terminated due to exceeding the displacement capacity of the test machine.

3.2.4. 625 Cycles

After 625 cycles (1250 h), the average of the maximum flexural loads of EB7 and EB8, which were kept under the standard laboratory conditions, increased by 38.2% over the control specimens. However, for those specimens exposed to 100% humidity at 100 °C after 625 cycles, significant reductions in the flexural strength were evident; the strength reductions were 16.5% and 41% for the 2 h-cycle specimens and for the zero-cycle specimens, respectively. For those exposed to 0% humidity at 100 °C, the strengths were lower than those of the 250-cycle specimens, but still higher than the control by 11.6 to 19.2%. The mode of failure of all these ten specimens was brittle flexural failure in a fashion similar to the control (see Figure 7).

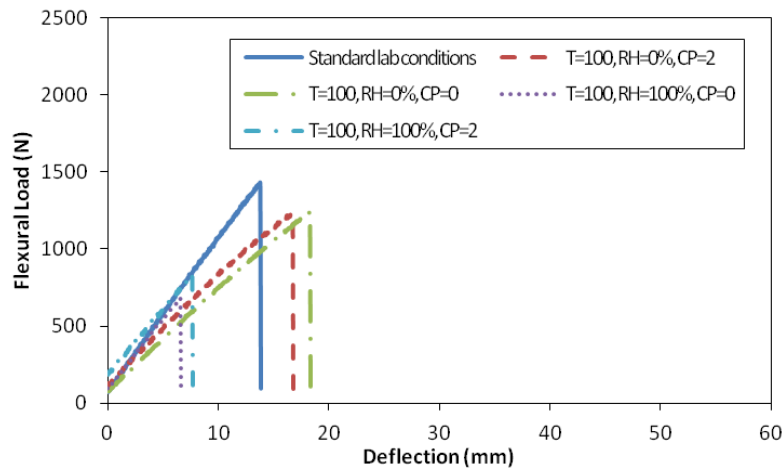


Figure 7. Flexural load-mid span deflection curves after 625 cycles under the conditions of 100 °C, humidity (0% and 100%), cycle period (Cp = 0 and 2).

3.3. 180 °C Conditioned Specimens

Additional flexural tests have been carried out for the specimens conditioned after 40 cycles, 100 cycles, 250 cycles, and 350 cycles (2-h cycle period only) at 180 °C. A constant and prolonged exposure to 180 °C was deemed too severe to reproduce the same types of deterioration as normally observed under the realistic environments. Hence, zero-cycle tests were not performed. In general, strength reductions to various degrees were observed, which will be discussed in the next section. The mode of failure of all specimens resembled the brittle flexural failure of the control (see Figure 8).

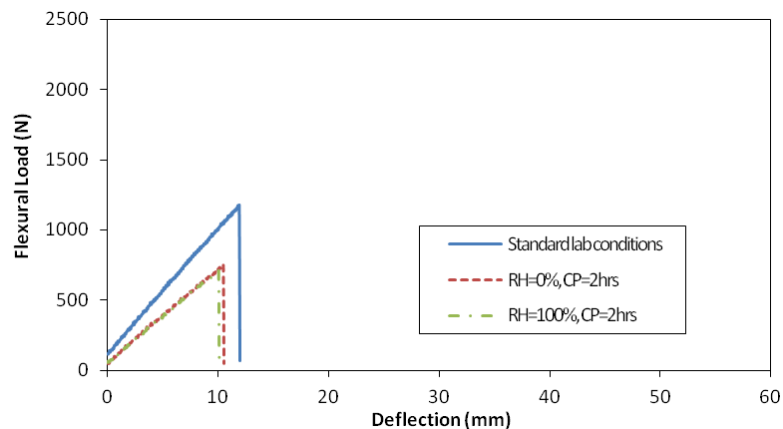


Figure 8. Flexural load-mid span deflection curves after 40 cycles under the conditions of 180 °C, 2-h cycle period, humidity (0% and 100%).

4. Discussions

4.1. Flexural Strength

Under the standard laboratory conditions, the maximum flexural loads increase with an increasing post curing time, which is related to the number of cycles. As shown in Figure 9, the increases in strength continue to rise from 9% after 80 h (40 cycles) to 56.7% after 1250 h (625 cycles).

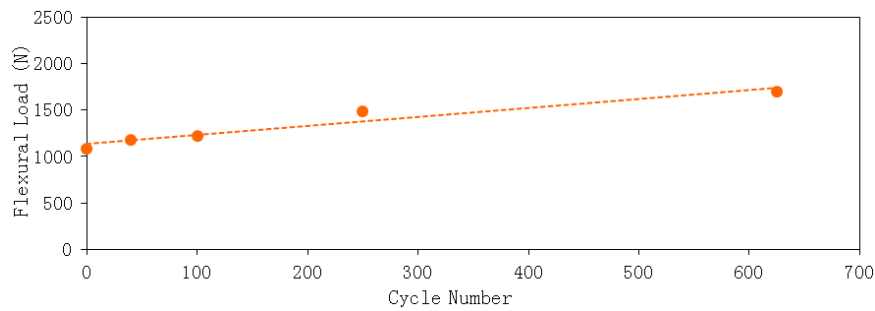


Figure 9. Maximum flexural loads vs. cycle numbers for the control specimens. Each cycle is equivalent to 2 h.

Under the conditions of a 100 °C dry environment (0% relative humidity), the 2-h cycle treatment produced higher strengths over time than that of the 0 cycle at the same numbers of cycles, ranging from 4.2% to 15% increases (Figure 10). However, the differences between these two cycle periods are insignificant. When the humidity level was 100%, the zero-cycle samples showed a slightly higher strength than the 2 h-cycle samples at the same cycle numbers, except for the 625-cycle specimens. The 2-h cycling treatment might allow the specimens to regain water during the lower temperature stage. Hence, the repeated sorption and desorption of water (water uptake and release) might cause more damage to the epoxy, leading to lower strengths. In general, the strength initially increased at a minor rate up to 250 cycles and the effect of moisture on strength was insignificant. After 250 cycles, a drop in strength was found in all cases, especially under the 100% humidity condition.

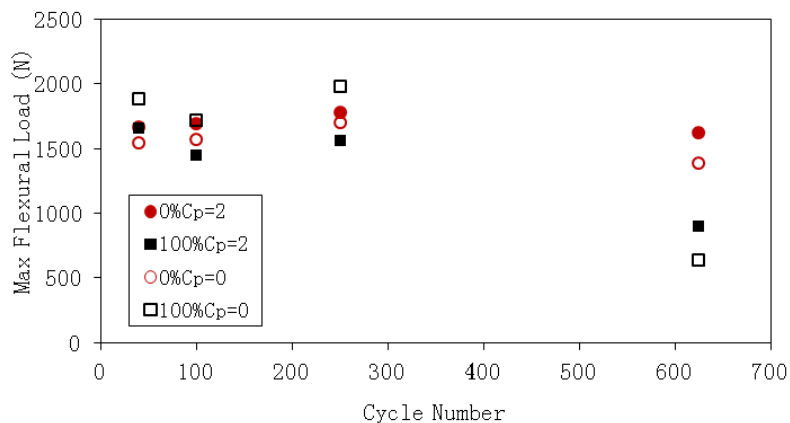


Figure 10. Max. flexural load vs. number of cycles under 100 °C but different humidity levels (0% and 100%) and different cycle periods ($C_p = 0$ and 2).

When the treatment temperature was raised to 180 °C, the maximum flexural loads initially increased up to 250 cycles, followed by a reduction for both the 0% and 100% humidity specimens in a manner similar to that of the 100 °C specimens (Figure 11). The differences between the 0% and 100% specimens were not significant. When comparing the effect of different temperatures, the 180 °C specimens showed strength reductions ranging from 39% to 62% in comparison to the corresponding 100 °C specimens.

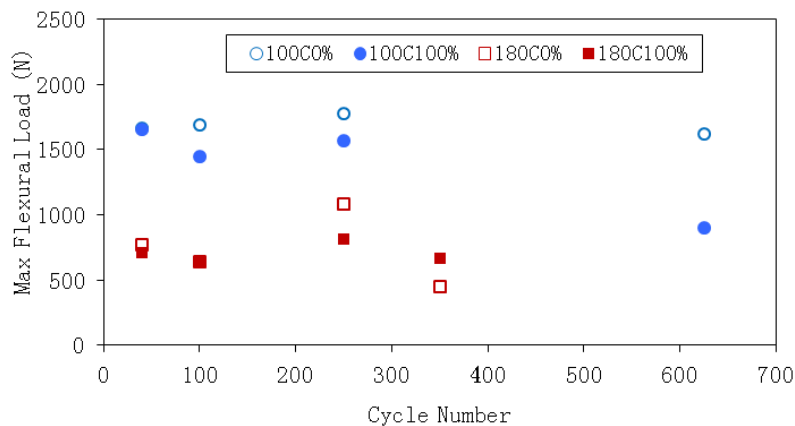


Figure 11. Max. flexural load vs. number of cycles at 100 °C and 180 °C ($C_p = 2$, 0% and 100% humidity).

4.2. Deflection

For the standard laboratory condition specimens, the maximum deflection increased continuously over time (Figure 12).

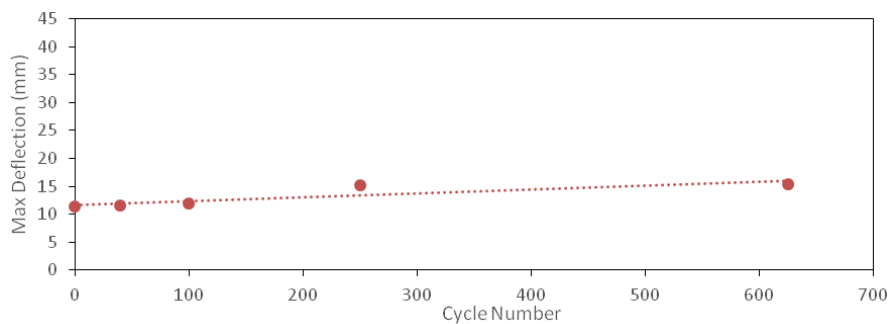


Figure 12. Max. deflection vs. number of cycles for the control specimens. Each cycle is equivalent to 2 h.

Under the conditions of a 100 °C dry environment (0% relative humidity), the 2-h cycle treatment produced slightly higher deflections over time than that of the 0 cycle at the same numbers of cycles (Figure 13). The deflection of the 100 °C-100% humidity specimens showed a trend similar to that of strength over the number of cycles. In all cases, a small reduction in deflection was observed up to 250 cycles. Beyond 250 cycles, the reductions accelerated, especially for the 100% humidity specimens. A 82% reduction was found from the 40-cycle to the 625-cycle specimen. It was noted that there is a peculiar drop in deflection from the 40-cycle to the 100-cycle specimen under the 0% humidity environments (Figure 13). Such abnormality is considered to be due to experimental errors, although the origin of the errors was not found.

When the treatment temperature was raised to 180 °C, the maximum deflections remained about the same throughout the entire test period (up to 350 cycles) for both 0% and 100% humidity specimens (Figure 14). In general, the 0% humidity specimens showed a slightly larger deflection capacity than the 100% specimens. When comparing the effect of different temperatures, the 180 °C specimens showed significant deflection reductions ranging from 63% to 83% in comparison to the corresponding 100 °C specimens. It must be noted that the maximum deflection of the 100 °C-100% humidity specimens after a long treatment period (625 cycles) approached that of the 180 °C specimens, showing a transition from ductile failure to brittle failure. After 625 cycles, the deflection of the 100 °C-0% humidity specimens was two to four times higher than that of the 100 °C-100% humidity specimens, which is

consistent with the strength data, as shown in Figure 11. It also confirmed that the repeated sorption and desorption of water during the temperature cycling might greatly damage the specimens.

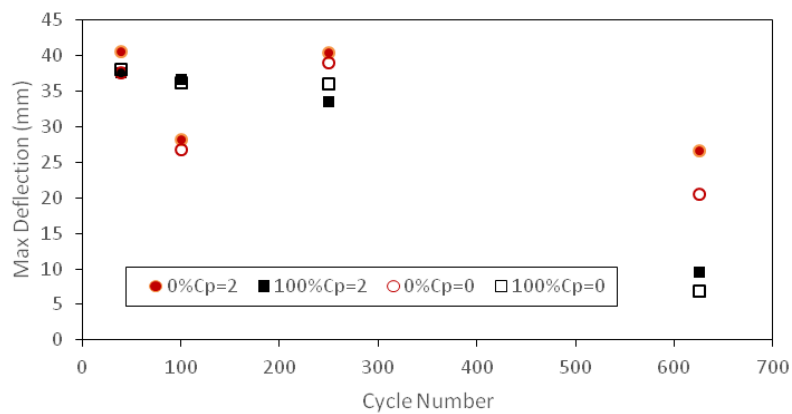


Figure 13. Max. deflection vs. number of cycles under 100 °C but different humidity levels (0% and 100%) and different cycle periods ($C_p = 0$ and 2).

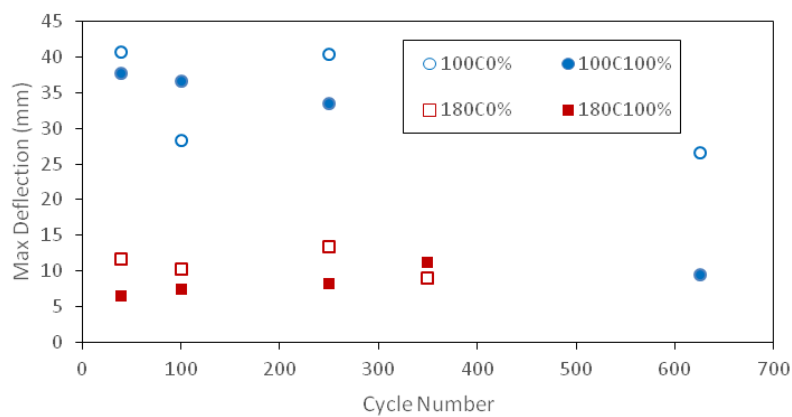


Figure 14. Max. deflection vs. number of cycles at 100 °C and 180 °C ($C_p = 2$, 0% and 100% humidity).

4.3. Apparent Stiffness

For the standard laboratory condition specimens, the apparent stiffness increased continuously over time (Figure 15).

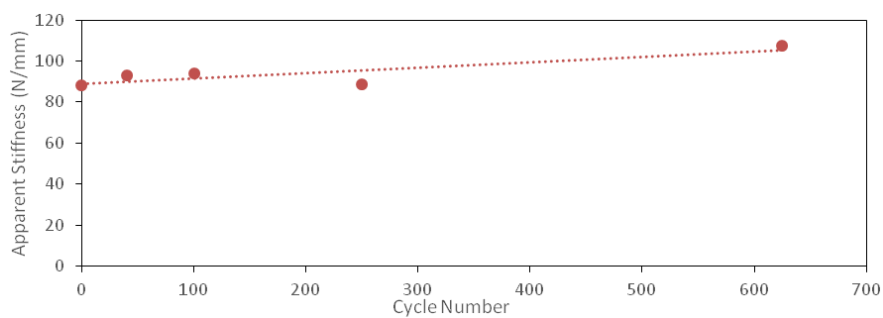


Figure 15. Apparent stiffness vs. number of cycles for the control specimens. Each cycle is equivalent to 2 h.

Under all the conditions of a 100 °C environment (0% or 100% relative humidity, 0 or 2 h cycle periods), the apparent stiffness quickly reduced by about (11–33)% from the stiffness of the control specimens within the first 40 cycles, and then remained about the same throughout the entire testing period (Figures 15 and 16). Although the data showed a large scattering, the general trend suggested that the level of humidity and the cycle period have an insignificant effect on the apparent stiffness. Therefore, in-field stiffness data must be interpreted with caution, since the strength reductions under the same environmental conditions were found to be severe, as reported above.

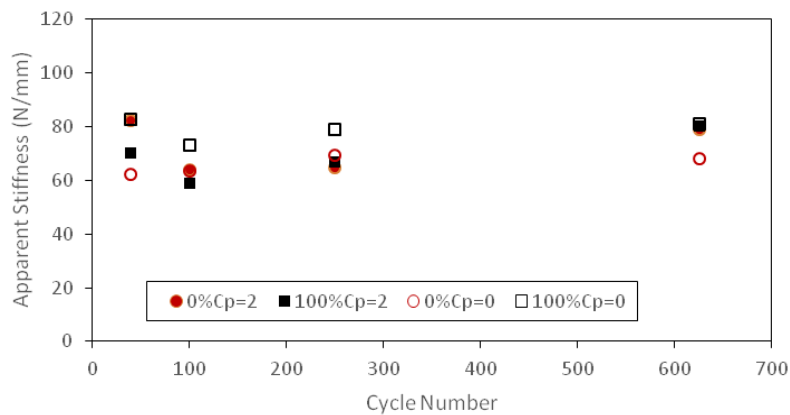


Figure 16. Apparent stiffness vs. number of cycles under 100 °C but different humidity levels and different cycle periods.

When the treatment temperature was raised to 180 °C, the apparent stiffness was similar to that of the 100 °C specimens and remained about the same throughout the entire test period (up to 350 cycles) for both the 0% and 100% humidity specimens (Figure 17).

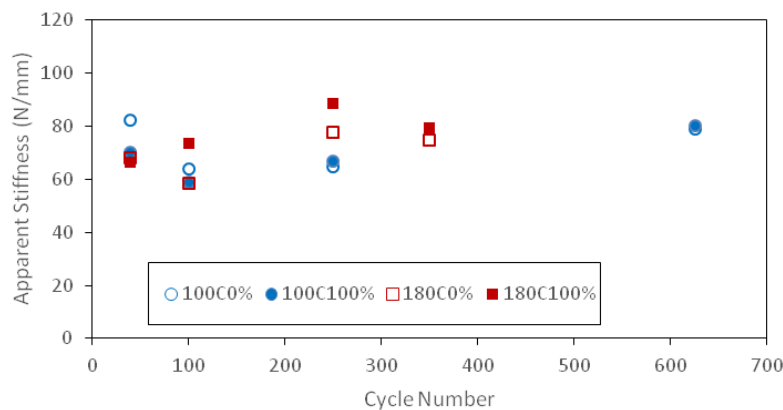


Figure 17. Apparent stiffness vs. number of cycles at 100 °C and 180 °C (Cp = 2, 0% humidity).

4.4. Mode of Failure

As shown in Table 3, there are two types of failure, brittle flexural failure and no failure, depending on the types of environmental exposure. No failure refers to those tests which were terminated due to exceeding the displacement limit of the MTS machine. Hence, no physical failure was observed. All the specimens either conditioned under the standard laboratory conditions or the 180 °C treatment showed brittle flexural failure. The specimens conditioned at 100 °C for a time period up to 250 cycles showed no failure for all but one specimen (at 40 cycles under the 0% humidity-zero cycle environment). However, a prolonged exposure at 100 °C regained the brittle flexural failure mode after 625 cycles (1250 h).

Table 3. Mode of failure under different environmental conditions.

Number Of Cycles	S.L.C. ¹	Mode of Failure					
		100 °C				180 °C	
		0% RH		100% RH		0% RH	100% RH
		Cp = 2	Cp = 0	Cp = 0	Cp = 2	Cp = 2	Cp = 2
0	Flexural	-	-	-	-	-	-
40	Flexural	x	Flexural	x	x	Flexural	Flexural
100	Flexural	x	x	x	x	Flexural	Flexural
250	Flexural	x	x	x	x	Flexural	Flexural
350	Flexural	-	-	-	-	Flexural	Flexural
625	Flexural	Flexural	Flexural	Flexural	Flexural	-	-

¹ S.L.C. is Standard laboratory conditions; (x) means no failure.

5. Conclusions

The following conclusions can be drawn from this study:

- (1) Under standard laboratory conditions, the maximum flexural loads, the maximum deflections, and the apparent stiffness all increase with an increasing time, which is related to the number of cycles. All specimens show brittle flexural failure.
- (2) The epoxy was sensitive to the effect of temperature. For all specimens conditioned at 100 °C, the strength initially increased up to 250 cycles. After 250 cycles, a decrease in strength was found. The 180 °C conditioned specimens showed strength reductions ranging from 39% to 62% in comparison to the corresponding 100 °C specimens at the same cycle numbers. In the case of 100 °C specimens, the majority of specimens showed very large deflections compared to the control due to a change in the failure mode from brittle to no failure; a small reduction in deflection was observed up to 250 cycles. Beyond 250 cycles, the reductions accelerated. On the other hand, the 180 °C specimens all show brittle failure; the maximum deflections were reduced by about 12–46% from that of the control. For all specimens, the apparent stiffness quickly reduced by about 11–33% from the stiffness of the control specimens within the first 40 cycles, and then remained about the same throughout the entire testing period.
- (3) The level of relative humidity appears to have an appreciable effect on the maximum strength and deflection of the epoxy specimens under both 100 and 180 °C environments. The combination of 100% humidity and long treatment periods produced a strong negative effect. After 625 cycle at 100 °C, the maximum deflection of the 0% humidity specimens was two to four times higher than that of the 100% humidity specimens.
- (4) The effect of temperature cycling vs. constant temperature at 100 °C was found to be insignificant in this study. When the maximum temperature was increased to 180 °C, the constant 180 °C environment would produce damage that was not likely to be observed during the service life of the FRP materials. Hence, such constant high temperature conditioning should not be employed in accelerating testing. On the other hand, a temperature cycling regime between room temperature and 180 °C appears to be adequate.
- (5) It should be noted that the abovementioned findings are based on the resin used in this study, which is common on the US market for impregnating FRP sheets. The interpretation of the hygrothermal effects on other resins must be made with caution.

Acknowledgments: The authors are grateful to the Wayne State University Library System for covering the costs to publish in open access.

Author Contributions: Abulgasem Mohamed Elarbi and Hwai-Chung Wu conceived and designed the experiments; Abulgasem Mohamed Elarbi performed the experiments; Abulgasem Mohamed Elarbi and Hwai-Chung Wu analyzed the data; Abulgasem Mohamed Elarbi wrote the paper.

Conflicts of Interest: The authors declare no conflict of interest.

References

1. Labossiere, P.; Neale, K.W.; Demers, M.; Picher, F. Repair of reinforced concrete columns with advanced composite materials confinement. In *Repair and Rehabilitation of the Infrastructure of the Americas*; Toutanji, H.T., Ed.; University of Puerto Rico: San Juan, Puerto Rico, 1995; pp. 153–165.
2. Seible, F.; Priestley, M.J.N.; Hegemier, G.A.; Innamorato, D. Seismic retrofit of RC columns with continuous carbon fiber jackets. *J. Compos. Constr.* **1997**, *1*, 52–62. [[CrossRef](#)]
3. ACI Committee 440. *Guide for the Design and Construction of Externally Bonded FRP System for the Strengthening Concrete Structures (ACI-440.2R-2000)*; American Concrete Institute (ACI): Farmington Hills, MI, USA, 2000.
4. Wu, H.C.; Sun, P.; Teng, J. Development of fiber reinforced cement based composite sheets for structural retrofit. *ASCE J. Mater.* **2010**, *22*, 572–579. [[CrossRef](#)]
5. Yalim, B.; Kalayci, A.S.; Mirmira, A. Performance of FRP-strengthening RC beams with different concrete surface profiles. *J. Compos. Constr.* **2008**, *12*, 626–634. [[CrossRef](#)]
6. Mikami, C.; Wu, H.C.; Elarbi, A. Effect of hot temperature on pull-off strength of FRP bonded concrete. *Constr. Build. Mater.* **2015**, *91*, 180–186. [[CrossRef](#)]
7. Triantafyllou, G.G.; Rousakis, T.C.; Karabinis, A.I. Axially loaded reinforced concrete columns with a square section partially confined by light GFRP straps. *J. Compos. Constr.* **2015**, *19*, 1. [[CrossRef](#)]
8. Foster, S.K.; Bisby, L.A. Fire survivability of external bonded FRP strengthening systems. *J. Compos. Constr.* **2008**, *12*, 553–561. [[CrossRef](#)]
9. ASTM D7522/D7522M-09. *Standard Test Method for Pull-Off Strength for Frp Bonded to Concrete Substrate*; American Society for Testing and Materials: Philadelphia, PA, USA, 2009.
10. Abanilla, M.A.; Li, Y.; Karbhari, V.M. Durability characterization of wet layup graphite/epoxy composites used in external strengthening. *Compos. Part B* **2006**, *37*, 200–212. [[CrossRef](#)]
11. Silva, M.A.G.; Biscaia, H. Degradation of bond between FRP and RC beams. *Compos. Struct.* **2008**, *85*, 164–174. [[CrossRef](#)]
12. Benzarti, K.; Chataigner, S.; Quiertant, M.; Marty, C.; Aubagnac, C. Accelerated ageing behavior of the adhesive bond between concrete specimens and CFRP overlays. *Constr. Build. Mater.* **2011**, *25*, 523–538. [[CrossRef](#)]
13. Wu, H.C.; Yan, A. Durability simulation of FRP bridge decks subject to weathering. *Compos. Part B* **2013**, *51*, 162–168. [[CrossRef](#)]
14. Karbhari, V.M. E-glass/vinyl ester composites in aqueous environments: Effects on short-beam shear strength. *J. Compos. Constr.* **2004**, *8*, 148–156. [[CrossRef](#)]
15. Rivera, J.; Karbhari, V.M. Cold-temperature and simultaneous aqueous environment related degradation of carbon/vinylester composites. *Compos. Part B* **2002**, *33*, 17–24. [[CrossRef](#)]
16. Jones, F.R. Durability of reinforced plastics in liquid environments. In *Reinforced Plastics Durability*; Pritchard, G., Ed.; Woodhead Publishing Company: Cambridge, UK, 1999; pp. 70–110.
17. Pérez-Pacheco, E.; Cauich-Cupul, J.I.; Valadez-González, A.; Herrera-Franco, P.J. Effect of moisture absorption on the mechanical behavior of carbon fiber/epoxy matrix composites. *J. Mater. Sci.* **2013**, *48*, 1873–1882. [[CrossRef](#)]
18. Hayes, M.F.; Bisby, A.; Beaudoin, Y.; Labossiere, P. Effects of freeze-thaw action on the bond of FRP sheets to concrete. *Canadian J. Civ. Eng.* **2000**, *27*, 949–959.
19. Birger, S.; Moshonov, A.; Kenig, S. The effects of thermal and hygrothermal ageing on the failure mechanisms of graphite-fabric epoxy composites subjected to flexural loading. *Composites* **1989**, *20*, 341–348. [[CrossRef](#)]
20. Haque, A.; Mahmood, S.; Walker, L.; Jeelani, S. Moisture and temperature induced degradation in tensile properties of kevlar-graphite/epoxy hybrid composites. *J. Reinf. Plast. Compos.* **1991**, *10*, 132–145. [[CrossRef](#)]
21. Ouyang, Z.; Wan, B. Modeling of moisture in FRP strengthened concrete specimens. *J. Compos. Constr.* **2008**, *12*, 425–434. [[CrossRef](#)]
22. Gartner, A.; Douglas, E.P.; Dolan, C.W.; Hamilton, H.R. Small beam bond test method for CFRP composites applied to concrete. *J. Compos. Constr.* **2011**, *15*, 52–61. [[CrossRef](#)]
23. Minnetyan, L.; Murthy, P.L.N.; Chamis, C.C. Progressive fracture in composite subjected to hygrothermal environment. *Int. J. Damage Mech.* **1992**, *1*, 60–79. [[CrossRef](#)]

24. Wu, H.C.; Fu, G.; Gibson, R.F.; Yan, A. Durability of FRP composite bridge deck materials under freeze-thaw and low temperature conditions. *J. Bridg. Eng.* **2006**, *11*, 443–451. [[CrossRef](#)]
25. ASTM D 790-07. *Standard Test Methods for Flexural Properties of Unreinforced and Reinforced Plastic and Electrical Insulation Materials*; American Society for Testing and Materials: Philadelphia, PA, USA, 2008.



© 2017 by the authors. Licensee MDPI, Basel, Switzerland. This article is an open access article distributed under the terms and conditions of the Creative Commons Attribution (CC BY) license (<http://creativecommons.org/licenses/by/4.0/>).